Assessing the effect ofseasonality onleaf and canopy spectra forthe discriminationof an alien tree species, *Acacia mearnsii,*from co-occurring native species using parametric and non-parametric classifiers

Cecilia Masemola[a, b], Moses Azong Cho[a, c,] Abel Ramoelo[d, e]

[a]Earth Observation Research Group, Natural Resources and Environment, Council for Scientific and Industrial Research, P O Box 395; Pretoria 0001; South Africa;

[b]College of Agriculture and Environmental Science, University of South Africa, P O Box 392, Pretoria, 0003, South Africa;

[c]Forest Science Postgraduate Programme, Department of Plant and Soil Science, Private Bag X20, University of Pretoria, Hatfield, 0028, South Africa;

[d]Vulnerability Assessment Centre, University of Limpopo, Sovenga, 0727, South Africa;

[e]Conservation Services, South African National Parks (SANParks), P.O.Box 787, Pretoria, 0001

Abstract

The tree *Acacia mearnsii* is native to south-eastern Australia but has become an aggressive invader in many countries. In South Africa, it is a significant threat to the conservation of biomes. Detecting and mapping its early invasion is critical. The current ground-based methods to map *A. mearnsii* are accurate but are neither economical nor practical. Remote sensing (RS) provides accurate and repeatable spatial information on tree species. The potential of RS technology to map *A. mearnsii* distributions remains poorly understood, mainly due to a lack of knowledge on the spectral properties of *A. mearnsii* relative to co-occurring native plants. We investigated the spectral uniqueness of *A. mearnsii* compared to co-occurring native plant species within the South African landscape. We explored full-range (400–2,500 nm), leaf and canopy hyperspectral reflectance of the species. The spectral reflectance was collected bi-weekly from 23 December 2016 and 31 May 2017. We conducted a time series analysis, to assess the effect of seasonality on species discrimination. For comparison, two classification models were employed: parametric interval extended canonical variate discriminant (iECVA-DA) and non-parametric random forest discriminant classifiers (RF-DA). The results of this study suggest that phenology plays a crucial role in discriminating between *A. mearnsii* and sampled species. The RF classifier discriminated *A. mearnsii* with slightly higher accuracies (from 92% to 100%) when compared with the iECVA-DA (from 85% to 93%). The study showed the potential of RS to discriminate between *A. mearnsii* and co-occurring plant species.

Keywords: *Acacia mearnsii,* extended canonical variates analysis, Random Forest, invasive tree species classification, linear discriminant analysis, leaf and canopy reflectance.

1. Introduction

Invasive alien plant (IAP) are of concern in ecological studies [1]. Invasion poses significant threats to the ecological integrity of terrestrial and aquatic ecosystems [2, 3]. The International Union for Conservation of Nature: Invasive Species Specialist Group (IUCN-ISSG) [4] classifies Australian *Acacia* species among the world's 100 worst IAP [1]. A native of south-eastern Australia, *Acacia mearnsii* (black wattle) has become an aggressive invader in many countries [5]. For example, it is a significant invader in the montane rainforest in Rwanda [6]. Moreover, [7] reported it to be the main invader in indigenous cork oak forests in Algeria. In South Africa, it is the most significant threat to the conservation of biomes as it has aggressively invaded grasslands [8, 9], indigenous forests [10], and watercourses [11]. The main environmental impacts of *A. mearnsii* include biodiversity loss; specifically by modifying the structure and composition of terrestrial and riparian inhabitants [2, 3] reduction of catchment and river water flows [12, 13] the functioning of ecosystems by changing the nitrogen cycle [14] and the intensification of wildfires [11]. Detecting and mapping its early invasion is critical for an effective management strategy.

Early invasion and rapid response require accurate, consistent and timely information on species distribution. Information on IAP species distribution has been successfully used to model risks and impacts of invasions at landscape [15, 16] and regional scales [17]. To understand the distribution patterns of *A. mearnsii*, spatial information of its occurrence is required. Currently, *A. mearnsii* mapping is based on ground survey methods and spatial interpolation techniques that approximate its presence at the un-sampled points [18]. The ground-based approach is accurate but is neither cost-effective nor practical. This approach also precludes accurate mapping of the species over a vast region [19]. In recent years, ecologists have embraced RS technology to map invasive species occurrences [1,7,14, 20].

RS provides a non-invasive and non-destructive means of obtaining continuous spatial coverage of the target species' distribution [19]. Over the years, RS data have been used to discriminate between invasive and native plant species in various ecosystems, for example, river estuaries [21], coastal dune ecosystems [24, 25, 26] and tropical rainforests [22, 23]. However, not all invasive species can be mapped using RS [30]. RS mapping of invasive species depends on their spectral separability from other native species in a heterogeneous species environment.

Previous studies showed that the spectral separability of species depend on the assumption that each species has a unique spectral signature, controlled by their distinctive structural and biochemical features [24-27,29,30]. For example, [29] reported separability between native and exotic trees based on their spectra reflectance differences in Hawaiian rainforest. Their study linked spectral separability of the species to variations in leaf pigment, nutrient and structural constituents. A study by [24-26] showed that absorption features for distinguishing native Mediterranean dune species correlate with the biochemical properties of the species (e.g. pigments, water, lignin and cellulose). According to [30], highly pubescent (hairy) plants reflected incident light energy very differently from the less hairy surrounding vegetation. Other research reported spectral distinction between nitrogen-fixing and non-fixing trees [23].

Acacia mearnsii, like other invasive species, possesses functional traits that may be different from those of native species. For example, *A. mearnsii* has been reported to have powerful competitive advantages due to high efficiency in the acquisition and use of nutrients specifically nitrogen [32]. The species has a rapid growth rate, sizeable aboveground biomass and associated leaf area when compared to indigenous vegetation [33]. Moreover, the species has pronounced hairy leaves which have been found to reflect incident light energy much differently from the less hairy surrounding vegetation [30]. Although spectral discernment of Australian Acacias from native species has been accomplished [24, 25, 26], the spectral separability between *A. mearnsii* and co-occurring species has not been meticulously investigated. There is thus no comprehensive regional spatial data of the occurrence of the species in South Africa, even though *A. mearnsii* has been rated to be the most aggressive alien species [32-34]. Therefore, the question is whether *A. mearnsii* could be discriminated from co-occurring native species based on leaf and canopy spectral information like other Australian acacias.

Hyperspectral data is known to provide detailed spectral information related to species-level chemical-structural properties [23]. The adjacent bands allow the detection of subtle spectral

differences between species that are otherwise masked by broadband sensors [23, 29, 36]. Hence, hyperspectral data have been used as an operational tool for early detection and modelling of future invasion risks [28, 37]. In Hawaii, RS tools have been used to develop invasive species monitoring strategies [38]. Spatially explicit *A. mearnsii* mapping models are hindered by the dearth of information concerning its spectral separability, what constitutes its spectral separability relative to adjacent species, and the appropriate spectral resolution required to provide accurate distribution maps [24-26]. Several studies have shown that comprehensive spectral libraries could give insights into the separability of target species [25, 40]. Subsequently, spectral libraries could be used for the prediction of future invasions and identifying priority areas for conservation [88, 89, 40]. This highlights the need for understanding the spectral characteristics of *A. mearnsii* when compared to that of co-occurring native species.

Although hyperspectral data have the prospects for quantifying spectral properties of plant species, its application precludes large area mapping due to a small swath width of the collected data [40]. Moreover, lower revisit frequencies limit the chance to capture the target species' spatial and phenological changes

[40]. Due to the rapid growth [6, 8, 41, 42] and spread [43] of *A. mearnsii,* hyperspectral sensors can hinder early detection and timely monitoring prospects. However, *A. mearnsii* tends to form large stands and patches [44], which makes it possible to detect the species using high spatial and satellite sensors with frequent revisiting time such as Multispectral Instrument (MSI) on-board Sentinel-2 [45, 46] and Operational Land Imager (OLI) on-board Landsat-8 satellite [45, 47]. The availability of space-borne sensors such as Sentinel-2 and Landsat-8 Operational Land Imager (OLI) could provide an opportunity to distinguish *A. mearnsii* at the landscape level. However, only a few studies have investigated the potential to map *A. mearnsii* using multispectral satellite data [48]. For this reason, we extended the research by including the multispectral dimension to the analysis. The present study aimed to explore:

(i) whether *A. mearnsii* is spectrally separable from the co-existing native species;

(ii) the best spectral wavelength regions for discriminating *A. mearnsii* from its co-occurring native species in South Africa using leaf and canopy spectral reflectance;

(iii) the optimal phenological period to separate *A. mearnsii* from its co-occurring species;

(iv) the potential of Landsat-8 OLI and Sentinel-2 spectral band configurations for discriminating *A. mearnsii* from co-occurring plant species

2. Methods and materials

2.1 Experimental setup and sampling

The research method chosen to meet the objectives of the study was an outdoor experiment with potted plants. The co-occurring species include *Dombeya tileacea, Olea africana, Dombeya rotundifolia, Euclea crispa, Vachellia karroo* and *Vachellia xanthophloea. A. mearnsii* and the co-occurring species show differences in their foliage structures as depicted in Fig. 1. Approximately 1-metre tall species were purchased from Nkosi Indigenous Plant Species Nursery based in KwaZulu-Natal, South Africa. The potted plants were left to grow outdoors on the campus of the Council for Scientific and Industrial Research (CSIR) for three months (1 September 2016 to 22 December 2016) before the start of the spectral data collection. The trees were randomly placed to allow the same distribution of energy and other resources. Due to the limited rainfall during this period, we watered the plants once a week from 1 September to 21 December 2016. The experiment took into consideration the soil type of the study area to be surveyed during data collection.

Species	Picture	Some characteristics
Acacia mearnsii		Evergreen tree, 6–20 m high. Fast-growing leguminous (nitrogen-fixing) tree. Leaves dark olive-green branchlets with all parts finely hairy. Leaflets short (1.5–4 mm). Flowering Aug–Sept.
Vachellia karroo		A deciduous tree (7–12 m). Leaves (pinnate pairs leaflets. Flowering Nov–April.
Vachellia xanthophloea		A deciduous tree (7–12 m). Leaves (pinnate pairs leaflets. Flowering November–April.
Euclea crispa		Variable short shrub to medium tree (8–20 m), Flowering December–May.
Dombeya tiliacea		Scrambling shrub tree (10 m). Spiralled, ovate leaves. Flowering March–August.
Dombeya rotundifolia		Small deciduous tree (5–10 m). Spiralled irregular lobed dark green leaves. Flowering July–September.
Olea Africana		Tree to 14 m tall in the forest. Opposite, decussate, shiny, leathery leaves. Flowering October–January.
Celtis Africana		A deciduous tree (30 m), smooth and slightly leathery leaves. Flowering August–October.

Fig. 1. Plant species used to explore spectral separability of *A. mearnsii* from native species

2.2 Canopy level spectra measurements

We conducted a total of nine sets of canopy radiance measurements on a biweekly basis from 23 December 2016 to 31 May 2017. They match the start and the end of the growing seasons in South Africa. The canopy measurements were carried out between 10:00 and 14:00 on cloud-free days. During the sampling campaign, we collected both leaf and canopy reflectance of the selected species between 350 and 2500 nm using an ASD FieldSpec FR 3 Spectroradiometer at 1 nm bandwidth (Analytical Spectral Devices Inc.,

Boulder, USA). We positioned the fibre optic (FOV 25°) at nadir and a height of approximately 30 cm above the undisturbed individual tree canopy.

Consequently, the field of view at the canopy level was circular, with a radius of 13.3 cm, and the field of view area was covered entirely by leaves to ensure standardised measurements. Furthermore, we eliminated the interference of the background (grass and bare ground) reflectance by placing the pot on a black sheet (board) [49]. We used a ladder for the canopy measurements to ensure that the entire canopy was covered to account for the canopy spectral variability. In order to get the canopy spectral data of each plant, we randomly took six radiance readings and calculated the average to get one canopy reflectance. Overall we collected 80 x 6 measurements per survey. To reduce the effects of changing atmospheric and solar conditions, the reflectance of a Spectralon white reference panel was recorded every 10-15 measurements. The reflectance of the individual tree was converted using a reference measurement for each sample by dividing the reflected target radiance by the irradiance of the white Spectralon® panel.

2.3 Leaf-level spectra measurement

After every canopy measurement, ten leaves per tree were randomly harvested and taken to a dark laboratory room with the walls and the ceiling coated with the black material. The dark room was used to ensure stable atmospheric and uniform illumination conditions [50-52]. We placed the leaves on a non-reflective black background surface to avoid the impact of external illumination. However, the leaflets of the pinnate leaves of *A. mearnsii, V. Karroo* and *V. Xanthophloea* (refer to Fig. 1) were smaller than the sensor FOV, and their reflectance measurements would therefore not be truly representative of the leaf morphology and biochemistry because the leaf area per unit surface would also impact the measured reflectance.

Consequently, we counteracted this effect by stacking the leaflets to simulate a continuous layer of leaves [53]. The fibre optic with a FOV of 25° was attached to the leaf clip and placed in a nadir position from approximately 4 cm above the leaves. However, in case of bigger leaves, no stacking of the leaves was done during spectra data collection. To capture the natural variations of leaf properties, five measurements were collected per leaf by repositioning the leaf clip at five different positions for each scan. The reflectance of the individual plant was obtained by averaging the collected spectra reflectance per plant. The resultant spectral database included that of *A. mearnsii* and seven grown native tree species.
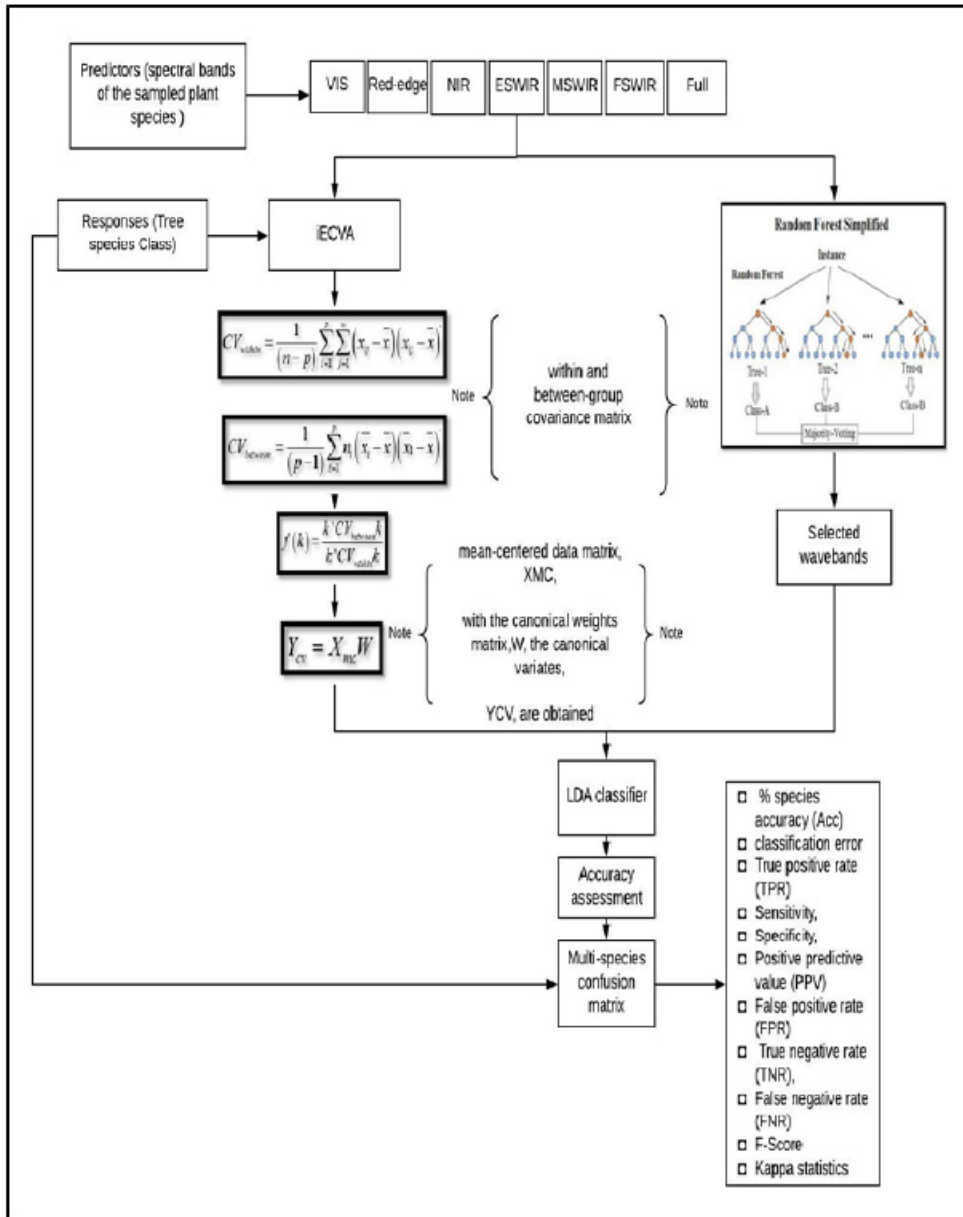
Fig. 2. Proposed method for distinguishing between A. mearnsii and sampled native species using leaf and canopy spectral reflectance.

2.4 Spectral reflectance pre-processing

The pre-processing of spectral reflectance was conducted using the Field Spectroscopy Facility (FSF) Post-Processing Toolbox (MATLAB toolbox) [54].

(*i*) the toolbox allowed for the exclusion of outliers caused by measurement errors and atmospheric interference;

(*ii*) the 350–399 nm bands were not included in the analysis, thus limiting the spectral range to the traditional visible (VIS) to shortwave infrared (SWIR) (400 nm to 2500 nm);

(*iii*) in the case of canopy spectra reflectance, we removed SWIR ranges with high noise that were identified through literature and visual inspection, that is, 1350–1460 nm and 1790–1960 nm [25].

After applying the pre-processing, 1759 canopy bands were left for analysis. Lastly, we eliminated sensor noise by using a moving Savitzky-Golay filter [55] with nine-point window size and second polynomial order. Furthermore, we explored various spectral transformation algorithms to evaluate the impact of spectral transformation on species discrimination. We considered the following methods: multiplicative scatter correction (MSC) [56], standard normal variation (SNV) [57] and first derivatives. The performance of the transformed data was then compared with that of the untransformed spectral dataset.

2.5 Simulation of Landsat-8 OLI and Sentinel-2 wavelengths

To investigate the potential of mapping *A. mearnsii* at the regional level using spaceborne sensors, we simulated Landsat-8 OLI and Sentinel-2 MSI data based on canopy spectral measurements using the respective pre-defined spectral response functions provided by the package 'hsdar'- CRAN.R-project.org [58] of R statistical software [59]. The resultant centre wavelengths were: Landsat 8 OLI (442.96 nm; 482.04 nm; 561.41 nm; 654.59 nm; 864 nm; 1609 nm and 2201 nm) and Sentinel-2 (490 nm; 560 nm; 665 nm; 705 nm; 740 nm; 785 nm; 842 nm, 1601 nm and 2190 nm).

2.6. Classification of plant species samples from leaf and canopy spectra data

The classification between *A. mearnsii* and sampled native species was based on multivariate Interval Extended Canonical Variable Analysis (iECVA) [60] and tree-based Random Forest discriminant analysis (RF-DA) [61, 62] methods. Fig. 2 summarises the methodology applied in this work. The analysis was carried out in Matlab using the ECVA toolbox available at http://www.models.life.ku.dk/source/. On the other hand, RF-DA applied for the classification between *A. mearnsii* and sampled native species were carried out using Matlab Fathom Toolbox by [61]. The toolbox is available at http://www.marine.usf.edu/user/djones/.

2.6.1 Interval Extended canonical variate analysis-discriminant analysis

The iECVA method [60] is a modified classical CVA. The modification was done to mitigate the shortcomings of standard canonical variates analysis (CVA) discriminant analysis methods. Unlike standard CVA, iECVA [60] can handle high dimensional dataset [65]. The iECVA [60] is a statistical method that finds multivariate directions that separate species classes, and, subsequently, reduces the dimensionality of the predictors. The iECVA [60] reduces data dimensionality using embedded interval partial least square (iPLS) [63] concepts. The concept of iPLS is used to select important spectral regions to separate the species. In a nutshell, iECVA technique focuses on the absorption area that contains the critical information that discriminates between species classes. The iECVA uses the mathematical foundation of CVA explained below.

CVA is the problem that finds a direction, k, which maximises the ratio of the within the group and the between-group covariance matrices as shown in (4). The method assumes that the matrix, X *(n, m)* represents the spectral reflectance to be categorised into the samples to target species, where *n* (samples from different species) and *m* (number of wavelengths) per species. The standard CVA finds the within (1) and between (2) covariate matrices on the assumption that all species are subject to the same variability.

$$CV_{within} = \frac{1}{(n-p)} \sum_{i=1}^{p} \sum_{j=1}^{n} \left(x_{ij} - \overline{x} \right)\left(x_{ij} - \overline{x} \right)' \tag{1}$$

$$CV_{between} = \frac{1}{(p-1)} \sum_{i=1}^{p} n_i \left(\overline{x_i} - \overline{x} \right)\left(\overline{x_1} - \overline{x} \right)' \tag{2}$$

CVA is the problem that assumes to find a direction, k, which maximises the ratio of the within-group and the between-group covariance matrices as shown in Eq 3. In the case where CV_{within} is a non-singular, the eigenvalue problem is possible and is calculated as shown in Eq 5. However, for a singular CV_{within}, left multiplication by the inverse of CV_{within} is impossible, and this becomes problematic when CVA is used for calibration of multi-collinearity data as CVA tends to break down.

$$f(k) = \frac{k'CV_{between}k}{k'CV_{within}k} \tag{3}$$

$$CV_{between}k = \lambda CV_{within}k \tag{4}$$

$$CV^{-}_{within}CV_{between}k = \lambda k \tag{5}$$

The breakdown problem of CVA in multi-collinearly data has been elucidated by the formulation of iECVA [55]. The iECVA assumes that the two groups shown in Eq.1 and Eq. 2 can be rewritten according to [56] in which the directions of the multi-group analysis are calculated as in Equation 6 and then transformed into multivariate regression problem as in Equation 7.

$$\left(\overline{x_1} - \overline{x_2}\right)\left(\overline{x_1} - \overline{x_2}\right)' k = \lambda CV_{within} k \tag{6}$$

$$Y_{cv} = X_{mc} W \tag{7}$$

Where Y_{cv} represents the columns of the differences between each group mean and the overall mean, $X_{mc,}$ is between groups covariance, W is the weights, while e is the residual matrix. The partial least squares regression (PLS2) is used as the regression technique to solve the regression equation for the multi-group and is shown in Equation 7. In this case, the number of weights calculated corresponds to the number of groups; the weights are sorted in descending order and introduced into Eq. 3 for an optimisation process. During optimisation, the weight with the lowest value is left out before application of the classifier. PLS2 is utilised to ensure that the space covered by the retained k-1 weights cover the full space of the solution [57]. The canonical variates are obtained by multiplying mean-centred data matrix with the canonical weights matrix. The resulting canonical variates are then used as an input to the LDA classifier [55]. The model has a built-in centring; the spectra were therefore not mean-centred prior application of the model.

2.6.2. Random forest-discriminant analysis

In this work, iECVA has been compared to the tree-based RF-DA. RF is the most used technique for tree discrimination [90]. It is used for feature selection, thus providing a better understanding of the spectral information variation among species. In contrast to parametric iECVA, the RF is a non-parametric decision tree based technique. The technique uses the majority vote of the ensemble of trees to identify the species class. The values of the number of variables that are randomly sampled as candidates at each split (*mtry*) and the number of trees to grow (*ntree*) parameters were identified based on algorithm tuning strategy. We searched for the optimal *mtry* band the *ntree* values using random search and grid search strategies. Subsequently, the most accurate value for *mtry* was ten. These parameters were tuned because of their importance in RF. The rest of the RF parameters were based on default values used by [61].

We trained the RF model using bootstrapped leaf and canopy reflectance corresponding to the species. To avoid the influence of both between-class and within-class disparities during classification, we iterated the model 100 times during fitting as recommended by [65]. During training, the feature selection and removal of the most correlated spectral wavebands were based on embedded feature section techniques within RF. According to [66], the selection of the features is based on the variables (wavebands) importance yielded by random forest. This approach identifies important variables based on randomisation [66] and estimations of out-of-bag error [66]. The detailed description of the method can be found in [66]. Similar to iECVA, the selected variables were then used as an input to the DA classification model also found in Fathom Toolbox for Matlab [61].

In classification problems, an imbalanced dataset may lead to the inadequate identification of the minority class. To avoid the problems related to the majority class on the classifier we used an equal number of samples per species. Moreover, we examined the relative importance of different parts of the spectrum for distinguishing between *A. mearnsii* and native species. Both leaf and canopy spectral reflectance were divided into visible (VIS, 400- 650nm), Red-edge (RE,651-750 nm), near-infrared (NIR, 751- 1300nm), early-shortwave-infrared (ESWIR, 1301-1460 nm), mid-shortwave-infrared (MSWIR, 1451-1789 nm) and far shortwave-infrared (FSWIR, 1901-2449 nm) subregions.

2.7. Evaluation of classifiers performance

Performances of these spectral regions were then assessed and compared to each other and with that of the model built using the full-spectra data also known as a global model using a multi-class confusion matrix (MCCM). The MCCM evaluates the model based on per species accuracy (Acc) in percentage as shown in (8), classification error, true positive rate (TPR), sensitivity, specificity, positive predictive value (PPV) (9), false positive rate (FPR), true negative rate (TNR), false negative rate (FNR), F-Score and Kappa statistics (10). As explained in [67], sensitivity represents the proportion of actual positives that are correctly identified by a classification model, whereas specificity is the percentage of the true negatives correctly identified by an iECVA-LDA model. The numerical values of sensitivity represent the probability that iECVA-LDA [60] model could identify individual species. The higher the values of sensitivity, the higher the chance that the model will discriminate that particular species from others. On the other hand, the specificity represents the probability of the iECVA-LDA to distinguish a specific species without giving false positive results. Also, the model calculates per species accuracy from the proportion of both true positive and true negative in the selected population. The maximum numerical values of 1.0 or 100% demonstrate that the species is strongly separable from other species [67]. It is noteworthy that high sensitivity or specificity does not necessarily imply that the accuracy of the classification is high as well [67]. As a result, we also used the coefficient statistic to measure if there was an actual agreement between predicted and observed species [67]. According to Cohen, we can interpret kappa statistics as follows: values $\leq 0\%$ are an indication of no agreement, 20–40% is considered fair, while values between 41–60% are moderate, 61–80% is substantial, and values between 81 and 100 indicate perfect agreement [68]. The probability that the classifiers discriminated the *A. mearnsii* better than the random chance has been demonstrated with the Z-score and associated P-value.

According to [69, 70], sensitivity is conceptually equivalent to the Producer's Accuracy. Moreover, assesses the probability that the species will be classified an *A. mearnsii* if it is *A. mearnsii*. Whereas, Specificity is a measure of the probability that a species class will not be predicted as *A. mearnsii* if it is not *A. mearnsii*.

$$\% Accuracy = \frac{obtained\ result\ -\ expected\ result}{expected\ result} *100$$

(8)

(9)

$$Specificity = \frac{TN}{TN + FP}$$

(9)

Where TP = number of true positive, that is correctly classified as correct species and FN = number of false negatives, that is, wrongly classified as species.

$$Kappa = \frac{\Pr(a) - \Pr(e)}{1 - \Pr(e)}$$

(10)

Where $\Pr(a)$ and $\Pr(e)$ represent the probability of species classification success and probability of classification success due to chance, respectively.

3. Results

3.1 The spectral separability between A. mearnsii and co-occurring native species at the leaf level

Among all the transformations spectral transformation methods, spectral separability between *A. mearnsii* and studied native species was slightly higher with Standard normal variate (SNV) processed reflectance. Therefore, only the results observed from SNV transformed spectra are presented. Nevertheless, spectral separability of the species showed the difference in phenological stages throughout the sampled growing season of the year. Figure 3 and Table I, indicate the phenological period that optimised the spectral separability between *A. mearnsii* and studied native species. The period is the transition from peak productivity to senescence in South Africa (Table I, March and April). As showed in Figure 3, the distribution patterns of the tree species in the two-dimensional canonical variate space of their leaf spectra reflectance displayed a tight grouping of *A. mearnsii* and a rather substantial overlap among native species.

The tree species discrimination using iECV-DA and RF-DA models produced the best result in the VIS, Red-edge, NIR and early shortwave infrared (ESWIR) spectral regions (Table I). From Table I, iECVA-DA and RF-DA yielded accuracies and kappa coefficient that ranged from 85–100% and 93 to100%, respectively (Table I). In comparison, the RF-DA model yielded somewhat slightly higher accuracies and kappa coefficient that ranged from 93% to100%. We also observed an enhanced separation between *A. mearnsii* and native species in May with RF-DA (Table I).

In addition to the classification models based on selected wavebands, the classification based on the full spectra data set showed a significant (p=0.0002) separation between *A. mearnsii* and the native species. The full spectra data produced higher accuracies than models with MSWIR and FSWIR wavebands

(Table I). The strong performance of full spectra data implies that both classifiers can deal very well with high spectral variability and multi-collinearity of the hyperspectral data. Overall there was greater spectral confusion among the native species. Hence, iECVA-DA and RF-DA classifiers produced significantly lower overall accuracies and kappa statistics that ranged from 31–52% and 20–51%, respectively (Table I).

A statistical comparison of the classifiers suggests that there is no significant difference between the iECVA-DA and RF-DA tree-based models (Z=0.335, p = 0.369). Moreover, both classifiers indicated statistically significant P-value < 0.0002, inferring both models discriminated *A. mearnsii* better than random chance.
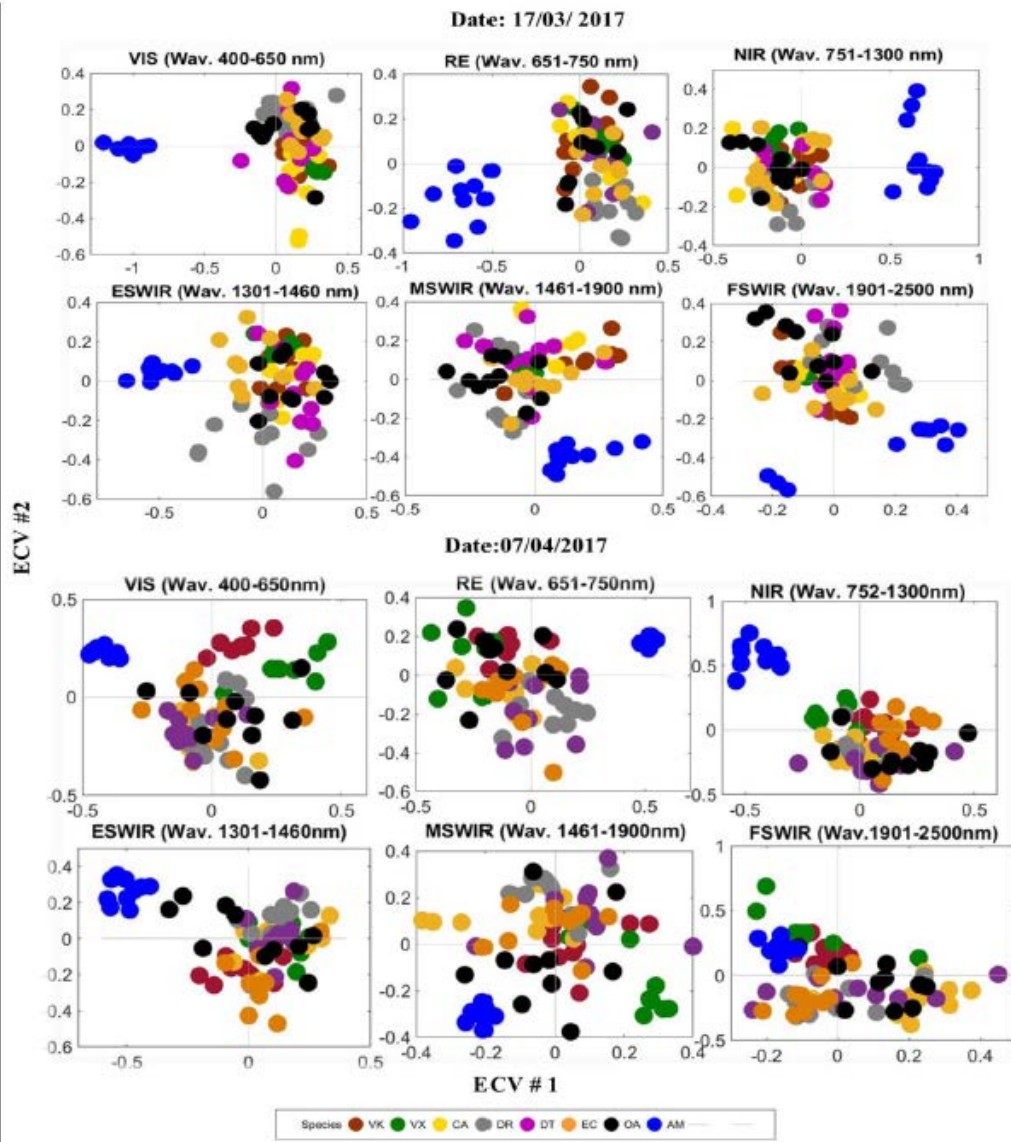
Fig. 3. Leaf scale distribution pattern of the studied plant species in ECV#1 versus ECV#2 2-D space of their leaf narrowband spectral regions during optimal separability period of *A. mearnsii*, The markers are: DT = *Dombeya tileacea*, OA = *Olea Africana*, DR = *Dombeya rotundifolia*, EC = *Euclea crispa*, VK = *Vachellia karroo*, and VX = *Vachellia xanthophloea*. ECV#1 ECV#1 and ECV#2 = first and second extended canonical variates, respectively.

TABLE I

LEAF SCALE STATISTICAL METRICS IN PERCENTAGE (%), FOR EACH SAMPLED SPECIES CLASS, YIELDED BY EACH EXPLORED SPECTRAL RANGE USING iECVA-LDA AND RF-DA = RANDOM FOREST-DISCRIMINANT ANALYSIS MODELS. THE BOLD RESULTS REPRESENT THE PERIOD WHERE *A. Mearnsii* IS HIGHLY DISCRIMINATED

Date	23/12/2016		13/01/2017		03/02/2017		24/02/2017		17/03/2017		07/04/2017		28/04/2017		12/05/2017		31/05/2017	
Accuracy metrics	RF	iECVA	RF	iECVA	RF	iECVA	RF	iECVA	RF	iECVA	RF	iECVA	RF	iECVA	RF	iECVA	RF	iECVA
Visible spectral region (VIS = 400-650 nm)																		
Acc (AM)	55%	53%	68%	67%	78%	60%	89%	85%	**93%**	**91%**	96%	95%	82%	74%	83%	67%	57%	27%
PPV (AM)	94%	68%	90%	71%	100%	68%	97%	78%	**100%**	**98%**	100%	100%	99%	69%	100%	72%	97%	60%
Kc (AM)	0.51	0.38	0.56	0.47	0.70	0.50	0.82	0.48	**0.90**	**0.87**	0.92	0.90	0.82	0.48	0.80	0.36	0.52	0.32
OAcc	36%	38%	34%	42%	39%	46%	59%	52%	**51%**	**49%**	50%	35%	60%	29%	40%	26%	24%	0%
Okc	0.31	0.29	0.39	0.34	0.32	0.27	0.53	0.34	**0.43**	**0.37**	0.43	0.42	0.54	0.27	0.29	0.22	0.24	0.17
Red edge spectral region (RE = 650-750 nm)																		
Acc (AM)	63%	39%	73%	44%	67%	58%	67%	67%	**91%**	**90%**	93%	91%	91%	77%	81%	67%	64%	0%
PPV (AM)	56%	46%	97%	60%	97%	66%	94%	58%	**97%**	**96%**	95%	99%	95%	55%	91%	76%	67%	25%
Kc (AM)	0.50	0.33	0.73	0.40	0.69	0.44	0.58	0.57	**0.86**	**0.87**	0.90	0.89	0.85	0.32	0.70	0.27	0.62	0.10
OAcc	39%	57%	45%	47%	35%	42%	44%	48%	**45%**	**31%**	39%	52%	66%	46%	32%	43%	19%	41%
Okc	0.29	0.37	0.37	0.42	0.30	0.42	0.34	0.28	**0.37**	**0.35**	0.37	0.46	0.58	0.33	0.25	0.39	0.24	0.22
Near Infrared spectral region (NIR = 751-1300 nm)											0.00							
Acc (AM)	27%	83%	33%	76%	46%	75%	60%	85%	**97%**	**96%**	100%	98%	83%	71%	89%	63%	46%	78%
PPV (AM)	90%	52%	90%	51%	94%	69%	40%	79%	**90%**	**98%**	96%	100%	100%	88%	100%	55%	94%	66%
Kc (AM)	0.18	0.66	0.22	0.65	0.45	0.70	0.30	0.73	**0.92**	**0.85**	0.96	0.92	0.90	0.53	0.85	0.48	0.45	0.37
OAcc	24%	26%	25%	36%	31%	38%	25%	33%	**25%**	**33%**	24%	42%	45%	23%	28%	38%	28%	31%
Okc	0.24	0.18	0.20	0.27	0.25	0.22	0.25	0.13	**0.20**	**0.27**	0.20	0.36	0.37	0.27	0.21	0.23	0.16	0.17
Early short-wave infrared (ESWIR = 1301-1460 nm)																		
Acc (AM)	0.33	0.51	0.54	0.67	0.64	0.60	0.44	0.79	**0.93**	**0.91**	0.95	0.98	0.62	0.83	0.77	0.71	0.60	0.13
PPV (AM)	0.90	0.65	0.96	0.56	0.96	0.68	0.92	0.82	**0.96**	**1.00**	0.94	1.00	0.97	0.90	1.00	0.65	0.94	0.48
Kc (AM)	0.22	0.57	0.55	0.62	0.62	0.68	0.34	0.68	**0.90**	**0.90**	0.91	0.90	0.56	0.63	0.71	0.57	0.54	0.45
OAcc	0.29	0.38	0.31	0.27	0.28	0.43	0.29	0.25	**0.31**	**0.33**	0.28	0.42	0.43	0.26	0.26	0.48	0.23	0.44
Okc	0.23	0.25	0.24	0.19	0.25	0.30	0.18	0.24	**0.24**	**0.27**	0.24	0.28	0.35	0.12	0.22	0.33	0.25	0.29
Mid shortwave Infrared region (MSWIR = 1461-1900 nm)																		
Acc (AM)	56%	30%	90%	67%	62%	50%	86%	75%	**94%**	**92%**	94%	93%	69%	49%	89%	40%	64%	30%
PPV (AM)	93%	65%	99%	69%	97%	72%	95%	77%	**99%**	**99%**	96%	99%	99%	65%	100%	44%	96%	36%
Kc (AM)	0.46	0.74	0.89	0.89	0.65	0.80	0.69	0.84	**0.89**	**0.84**	0.90	0.88	0.66	0.53	0.82	0.31	0.62	0.29
OAcc	34%	37%	48%	32%	26%	35%	28%	43%	**48%**	**52%**	26%	46%	36%	44%	36%	45%	33%	25%
Okc	0.28	0.39	0.43	0.64	0.21	0.48	0.26	0.61	**0.43**	**0.53**	0.21	0.58	0.29	0.59	0.32	0.59	0.28	0.45
Far short-wave infrared (FSWIR = 1901-2500 nm)																		
Acc (AM)	64%	50%	73%	44%	69%	33%	73%	53%	**83%**	**88%**	94%	91%	82%	43%	82%	25%	44%	17%
PPV (AM)	96%	57%	97%	51%	99%	48%	97%	68%	**97%**	**88%**	96%	95%	99%	57%	99%	35%	92%	19%
Kc (AM)	0.62	0.39	0.73	0.40	0.76	0.28	0.73	0.51	**0.77**	**0.87**	0.88	0.89	0.78	0.34	0.84	0.23	0.34	0.12
OA	44%	26%	41%	32%	31%	35%	40%	42%	**41%**	**51%**	26%	46%	43%	42%	41%	40%	30%	39%
OKc	0.36	0.34	0.32	0.16	0.24	0.13	0.30	0.19	**0.32**	**0.34**	0.21	0.33	0.34	0.25	0.33	0.17	0.20	0.23
Full spectral (400nm-2500nm)																		
Acc (AM)	67%	66%	67%	63%	69%	77%	86%	84%	**95%**	**90%**	100%	99%	90%	77%	80%	62%	69%	26%
PPV (AM)	90%	99%	97%	58%	99%	64%	95%	78%	**100%**	**95%**	100%	90%	99%	68%	97%	72%	93%	89%
Kc (AM)	0.58	0.48	0.54	0.57	0.66	0.62	0.79	0.64	**0.86**	**0.87**	0.95	0.94	0.85	0.40	0.76	0.31	0.58	0.29
OAcc	28%	35%	24%	45%	28%	36%	38%	25%	**47%**	**35%**	20%	45%	42%	25%	36%	37%	31%	32%
Okc	0.34	0.34	0.36	0.16	0.27	0.13	0.23	0.19	**0.33**	**0.34**	0.24	0.33	0.33	0.25	0.24	0.17	0.26	0.23

3.2 Canopy level spectral separability of A. mearnsii among co-occurring native species

At canopy level, similar spectral dissimilarities as that of leaf spectral data were observed between *A. mearnsii* and native species with an overall best discrimination accuracy between March and April (Table II). The ECV plots (Fig. 4) showed a clear separation between *A. mearnsii* and native species. Interestingly, upscaling from leaf to canopy level slightly increased the spectral variation between *A. mearnsii* and native species in the VIS, red-edge, NIR and ESWIR reflectance bands (Table II), irrespective of the classifier used. The iECVA-DA and RF-DA accuracies and Kappa statistics ranged from ranged from 92–100% and 93–100%, respectively (Table II). Contrary to iECVA-DA, RF-DA produced slightly higher accuracies in RE, NIR and ESWIR reflectance during the senescence-winter transition period, April-May (Acc(AM) = 83-95%, Kcc (AM)=0.75 -0.83).

Overall accuracies were significantly low which could be attributed to the strong spectral reflectance confusion between native species as demonstrated in Fig. 4. The use of the whole wavelength range (400–2,500 nm) yielded significant ($p=0.0001$) high accuracy for *A. mearnsii*, regardless of classifier employed. As opposed to iECVA-DA, at both leaf and canopy level, the spectral separability between *A. mearnsii* and native species was also clearly expressed in May (Table I and II) with RF-DA.
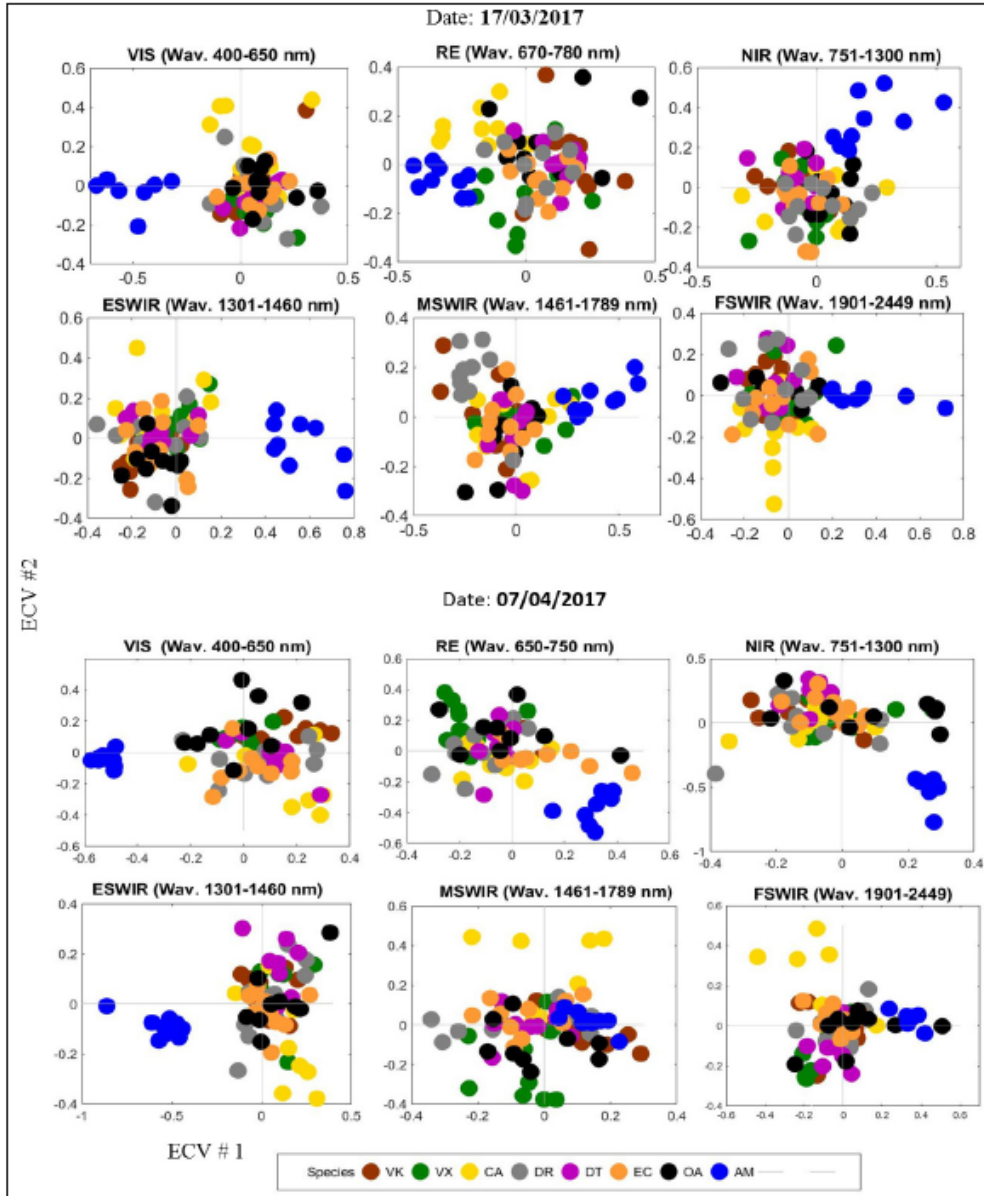
Fig. 4. Canopy level distribution pattern of the studied plant species in ECV#1 versus ECV#2 2-D space of their narrowband spectral regions during the optimal *A. mearnsii* separability period concerning canopy spectral reflectance. DT = *Dombeya tileacea*, OA = *Olea africana*, DR = *Dombeya rotundifolia*, EC = *Euclea crispa*, CA = *Celtis africana*, AM = *Acacia mearnsii*, VK = *Vachellia karroo*, and VX = *Vachellia xanthophloea*. While VIS = visible, RE = Red-edge, NIR = near-infrared, ESWIR = early shortwave-infrared, MSWIR = mid-shortwave-infrared, and FSWIR= are far shortwave-infrared, ECV#1 and ECV#2 = first and second extended canonical variates, respectively.

CANOPY-SCALE STATISTICAL METRICS FOR EACH SAMPLED SPECIES CLASS YIELDED BY EACH EXPLORED CANOPY SPECTRAL RANGE USING iECVA-LDA AND RF-DA = RANDOM FOREST-DISCRIMINANT ANALYSIS MODELS. THE BOLD RESULTS REPRESENT THE PERIOD WHERE A. Mearnsii IS HIGHLY DISCRIMINATED. AM = A. Mearnsii, CA = Celtis Africana, DT = Dombeya Tileacea, OA = Olea Africana, DR = Dombeya Rotundifolia, EC = Euclea Crispa, VK = Vachellia Karroo, AND VX = Vachellia Xanthophloea. WHERE ACC = ACCURACY, Kc = KAPPA COEFFICIENT, OACC = OVERALL ACCURACY, OKc = OVERALL KAPPA COEFFICIENT, PPV = POSITIVE PREDICTIVE VALUE

Date / Accuracy metrics	23/12/2016 RF	iECVA	13/01/2017 RF	iECVA	03/02/2017 RF	iECVA	24/02/2017 RF	iECVA	17/03/2017 RF	iECVA	07/04/2017 RF	iECVA	28/04/2017 RF	iECVA	12/05/2017 RF	iECVA	31/05/2017 RF	iECVA
Visible spectral region (VIS = 400-650 nm)																		
Acc (AM)	55%	53%	68%	67%	78%	60%	89%	83%	93%	91%	96%	95%	82%	74%	83%	67%	57%	27%
PPV (AM)	94%	68%	90%	71%	100%	68%	97%	78%	100%	98%	100%	100%	99%	69%	100%	72%	97%	60%
Kc (AM)	0.51	0.38	0.56	0.47	0.70	0.50	0.82	0.48	0.90	0.87	0.92	0.90	0.82	0.48	0.80	0.36	0.52	0.32
OAcc	36%	38%	34%	42%	32%	27%	59%	52%	51%	49%	50%	35%	60%	29%	40%	26%	24%	0%
Okc	0.31	0.29	0.39	0.34	0.32	0.27	0.53	0.34	0.43	0.37	0.43	0.42	0.54	0.27	0.29	0.22	0.24	0.17
Red edge spectral region (RE = 650-750 nm)																		
Acc (AM)	63%	39%	73%	44%	67%	58%	67%	67%	91%	90%	93%	91%	91%	77%	81%	67%	64%	0%
PPV (AM)	56%	46%	97%	60%	97%	66%	94%	58%	97%	96%	95%	99%	95%	55%	91%	76%	67%	25%
Kc (AM)	0.50	0.33	0.73	0.40	0.69	0.44	0.58	0.57	0.86	0.87	0.90	0.89	0.85	0.32	0.70	0.27	0.62	0.10
OAcc	39%	57%	45%	47%	30%	42%	44%	48%	45%	31%	39%	52%	66%	46%	32%	39%	19%	41%
Okc	0.29	0.37	0.37	0.42	0.30	0.42	0.34	0.28	0.37	0.35	0.37	0.46	0.58	0.33	0.25	0.39	0.24	0.22
Near Infrared spectral region (NIR = 751-1300 nm)																		
Acc (AM)	27%	83%	33%	76%	46%	75%	60%	85%	97%	96%	100%	98%	83%	71%	89%	63%	46%	78%
PPV (AM)	90%	52%	90%	51%	94%	69%	40%	79%	90%	98%	96%	100%	100%	88%	100%	55%	94%	66%
Kc (AM)	0.18	0.66	0.22	0.65	0.45	0.70	0.30	0.73	0.92	0.85	0.96	0.92	0.90	0.53	0.85	0.48	0.45	0.37
OAcc	24%	26%	25%	36%	25%	38%	25%	33%	25%	33%	24%	42%	45%	23%	28%	38%	28%	31%
Okc	0.24	0.18	0.20	0.27	0.25	0.22	0.25	0.13	0.20	0.27	0.20	0.36	0.37	0.27	0.21	0.23	0.16	0.17
Early short-wave infrared (ESWIR = 1301-1460 nm)																		
Acc (AM)	0.33	0.51	0.54	0.67	0.64	0.60	0.44	0.79	0.93	0.91	0.95	0.98	0.62	0.83	0.77	0.71	0.60	0.13
PPV (AM)	0.90	0.65	0.96	0.56	0.96	0.68	0.92	0.82	0.96	1.00	0.94	1.00	0.97	0.90	1.00	0.65	0.94	0.48
Kc (AM)	0.22	0.57	0.55	0.62	0.62	0.68	0.34	0.68	0.90	0.90	0.91	0.90	0.56	0.63	0.71	0.57	0.54	0.45
OAcc	0.29	0.38	0.31	0.27	0.28	0.43	0.29	0.25	0.31	0.33	0.28	0.42	0.43	0.26	0.26	0.48	0.23	0.44
Okc	0.23	0.25	0.24	0.19	0.25	0.30	0.18	0.24	0.24	0.27	0.24	0.28	0.35	0.12	0.22	0.33	0.25	0.29
Mid shortwave Infrared region (MSWIR = 1461-1900 nm)																		
Acc (AM)	56%	30%	90%	67%	62%	50%	86%	75%	94%	92%	94%	93%	69%	49%	89%	40%	64%	30%
PPV(AM)	93%	65%	99%	69%	97%	72%	95%	77%	99%	99%	96%	99%	99%	65%	100%	44%	96%	36%
Kc (AM)	0.46	0.74	0.89	0.89	0.65	0.80	0.69	0.84	0.89	0.84	0.90	0.88	0.66	0.53	0.82	0.31	0.62	0.29
OAcc	34%	37%	48%	32%	21%	48%	28%	43%	48%	52%	26%	46%	36%	44%	36%	45%	33%	25%
Okc	0.28	0.39	0.43	0.64	0.21	0.48	0.26	0.61	0.43	0.53	0.21	0.58	0.29	0.59	0.32	0.59	0.28	0.45
Far short-wave infrared (FSWIR = 1901-2500 nm)																		
Acc (AM)	64%	50%	73%	44%	69%	33%	73%	53%	83%	88%	94%	91%	82%	43%	82%	25%	44%	17%
PPV (AM)	96%	57%	97%	51%	99%	48%	97%	68%	97%	88%	96%	95%	99%	57%	99%	35%	92%	19%
Kc (AM)	0.62	0.39	0.73	0.40	0.76	0.28	0.73	0.51	0.77	0.87	0.88	0.89	0.78	0.34	0.84	0.23	0.34	0.12
OA	44%	26%	41%	32%	24%	13%	40%	42%	41%	51%	26%	46%	43%	42%	41%	40%	30%	39%
OKc	0.36	0.34	0.32	0.16	0.24	0.13	0.30	0.19	0.32	0.34	0.21	0.33	0.34	0.25	0.33	0.17	0.20	0.23
Full spectral (400nm-2500nm)																		
Acc (AM)	67%	66%	67%	63%	69%	77%	86%	84%	95%	90%	100%	99%	90%	77%	80%	62%	69%	26%
PPV (AM)	90%	99%	97%	58%	99%	64%	95%	78%	100%	95%	100%	90%	99%	68%	97%	72%	93%	89%
Kc (AM)	0.58	0.48	0.54	0.57	0.66	0.62	0.79	0.64	0.86	0.87	0.95	0.94	0.85	0.40	0.76	0.31	0.58	0.29
OAcc	28%	35%	24%	45%	28%	36%	38%	25%	47%	35%	20%	45%	42%	25%	36%	37%	31%	32%
Okc	0.34	0.34	0.36	0.16	0.27	0.13	0.23	0.19	0.33	0.34	0.24	0.33	0.33	0.25	0.24	0.17	0.26	0.23

3.3 Upscaling in situ canopies spectral to Sentinel-2 and Landsat-8 OLI bands

Table III shows results from using simulated Landsat 8 OLI and Sentinel-2 MSI data. The results of Sentinel-2 MSI shows comparable results with that of Landsat 8 OLI regarding discriminating between *A. mearnsii* and sampled native species. Both spectral datasets indicated high discrimination of the *A. mearnsii*. Sentinel-2 MSI yielded a percentage Acc (AM) of 95.52 and Kcc (AM) of 0.90, whereas Landsat-8 OLI spectral data achieved % Acc = 93.38 and Kcc of 0.88.

Although both classifiers selected the same variables, RF discriminated *A. mearnsii* with slightly lower Acc and Kcc (AM) values (Table III). Both classifiers selected the same best predictor variables (Table III), where SWIR and NIR showed to be important for Sentinel-2 MSI and Landsat 8 OLI (Table III). Also, red-edge (783 nm) and red-edge (707 nm) bands were selected as best the predictor variables for Sentinel-2. Furthermore, Red (654 nm) was selected for Landsat 8 OLI.

Models	RF		iECVA	
Accuracy metrics	S2-MSI	L8-OLI	S2-MSI	L8-OLI
Acc(AM)	92%	90%	95%	93%
PPV(AM)	100%	94%	100%	97%
Kc(AM)	0.89	0.89	0.90	0.88
OAcc	44%	45%	62%	57%
OKc	0.31	0.40	0.56	0.46
Important wavelengths	Red (665 nm), RE (783 nm), RE (707nm), NIR (835.6 nm) and SWIR (1610 nm)	Red (654.59 nm), NIR (864nm) and SWIR-2200nm	Red (665 nm), RE (783 nm), RE (707nm), NIR (835.6 nm) and SWIR (1610 nm)	Red (654.59nm), NIR (864nm) and SWIR-(2200nm)

4 Discussion

This study investigated the separability of *A. mearnsii* from co-occurring native species using both leaf and canopy hyperspectral reflectance. Spectral information of the species has been used successfully to discriminate invasive species from their co-occurring plant species [22, 23] but no study has been done for distinguishing invasive *A. mearnsii* among co-occurring native species in the South African landscape. This study demonstrated for the first time the utility of the iECVA-LDA classifier for classification of vegetation species. We also compared the ability of the iECVA-LDA classifier to discern species with that of RF-DA classifier. The results from our study suggest that *A. mearnsii* is distinguishable from native species. However, seasonal shifts showed to be important in separating between species. Our results corroborate those from [22] and [23] studies that have found the high spectral separation between invasive and native species due to phenology.

In this study, the most significant spectral differences between *A. mearnsii* and other species was observed for the March and April reflectance data at both leaf and canopy levels. In Southern Africa, March to April is the transition period from vegetation peak productivity to senescence [71] and [72]. The high separability of *A. mearnsii* during the summer-autumn transition period could be attributed to the fact that the species is an evergreen leguminous species [23, 71, 73]. According to [73], the canopy of evergreen

species remains relatively stable throughout the growing cycle. Thus during leaf fall and senescence evergreen species tends to exhibit a more traditional leaf strategy with higher leaf biomass and longer leaf lifespan when compared to deciduous plants.

Consequently, high biomass enhances the spectral separability between evergreen and deciduous tree, particularly during leaf senescence period [74]. As reported by [73], tree species that vary in leaf habit (deciduous and evergreen) have different leaf chemical and physiological leaf traits. Their study reported differences in the amount of nutrients per leaf area between evergreen and deciduous savannah species. Likewise [23] and [71] observed spectral disparities between deciduous and native species due to variations in structural and biochemical constituents during the transition period from March to April (peak productivity to senescence). The current study corroborates [73] because it demonstrated spectral information (such as biochemical and structural traits) shifts between *A. mearnsii* and sampled native species when conditions were unfavourable for the growth of native deciduous species.

4.1. Optimal spectral regions for species differences

The full spectrum (400–2500 nm) has been widely used for discriminating vegetation species [24, 25, 26, 29, 31]**.** Among explored hyperspectral regions, VIS, Red-edge, NIR and ESWIR from both leaf and canopy levels were significant in this study. The performance observed from regions above confirmed the results of [23] and [36] in which infrared region (680-1080 nm), VIS (400-650nm) and SWIR (1300-2500 nm) were the best regions for discriminating between native and invasive Hawaiian tree species. At the leaf level, the red edge spectral range did not contribute as much as VIS, NIR and ESWIR to distinguish between *A. mearnsii* from the native species. However, the red edge extracted from canopy spectra performed better than the MSWIR (1461-1789 nm) and FSWIR (1952-2449 nm). Substantial differences in the VIS, RE, NIR and ESWIR points to high disparities in biochemical and other properties that have an impact on the spectral signature in these regions between *A. mearnsii* and the native species. In the visible wavelengths regions, the spectral disparities between species are associated with differences in pigments concentration, mainly leaf chlorophyll. Numerous studies have shown that the RE region has a strong correlation with foliar chlorophyll and nitrogen content [77, 78].

Strong separability in the visible and the RE region of the spectrum, thus implies significant variation in nitrogen and chlorophyll content between *A. mearnsii* and studied native species. This study corroborates findings from [37] which indicated that there is a strong distinction in leaf traits between native and invasive Australian *Acacia* species. Australian acacias are nitrogen fixers [26,33], as such, they tend to have a more considerable amount of leaf N when compared to co-occurring non-N2-fixing trees and shrubs. As a result, it is not clear whether observed spectral differentiation at the visible regions is due to chlorophyll or leaf nitrogen as the two traits are strongly correlated.

Also, notable spectral reflectance differences exist between *A. mearnsii* and the rest of the trees in the SWIR part of the spectrum. The difference between an Australian *Acacia* spp and non-acacias species in the SWIR part of the spectrum is due to the differences in condensed tannin contents [24, 26]. Strong dissimilarities between the species in the SWIR spectral regions of the spectrum could suggest high nitrogen variations between species because it is highly correlated with N-H and C-H vibrations of proteins. Moreover, SWIR was found to be necessary for the discrimination of species based on leaf tannin content, which has been shown to vary between invasive Australian acacias and non-invasive species. For example, [24] discriminated *Acacia longifolia* using four SWIR wavelength regions (1360–1450 nm and 1630–1740 nm) due to their high correlation with tannin concentration. According to [75, 76] the dissimilarities at the SWIR could be attributed to the fact that wavelengths related to tannin are linked to the molecular vibration such as bending and broadening of C-H, C-O and O-H bonds and their overtones.

Substantiating the studies by [23, 36, 77], we observed disparities in discrimination abilities between leaf and canopy spectral. As in [23] the canopy level spectra showed a higher discrimination performance compared to leaf spectra. The difference in discrimination abilities among spectral regions, notably VIS and red edge at leaf and canopy levels, highlights the significance of scaling up the leaf-level spectral to the canopy level for species discrimination, as emphasised by [36,79]. Also, [29] showed improvement in differentiating species from canopy spectra, as compared to the leaf level. Moreover, [79] linked the disparities between leaf and canopy red edge spectra in discriminating species to the fact that canopy reflectance affords extra information, such as leaf orientation, leaf clumping and colour of twigs. On the other hand low separability in MSWIR and FSWIR spectral domains could be suggesting that the differences in leaf and canopy water content did not contribute significantly to spectral separability.

Furthermore, strong distinctions demonstrated at the NIR indicate differences in structural and physiological attributes in tannin contents [24]. The invasive *Acacia longifolia*, native to south-eastern Australia has been spectrally distinguished from native species based on its structural, secondary metabolites [24,26] and biochemical traits [26].

In general, physio-chemical traits dissimilarities between Australian acacia and studied native trees can be derived from their spectral reflectance data. The identified spectral regions from this study could be useful in providing scientific guidance for the development of tailor-made species mapping platforms like

unmanned aerial vehicle (UAV) [80, 81]. These platforms have been shown to offer a cost-effective solution to address the challenge of monitoring invasions [82].

4.2 Species discrimination based on simulated Sentinel-2 MSI and Landsat-8 OLI

In general, *A. mearnsii* is separable from sampled native species with both Landsat 8 OLI and Sentinel-2 MSI. Both Landsat-8 OLI and Sentinel-2 simulated data could discriminate over 90% of *A. mearnsii* among co-occurring species. Our results substantiate those of [83] in which both Sentinel-2 MSI and Landsat-8 OLI classified subtropical trees. Similar to studies by [84, 85] and [86], the current study found critical spectral regions for optimal discrimination of *A. mearnsii* in the red edge, NIR and SWIR for Sentinel-2 and NIR and SWIR for Landsat-8 OLI. Likewise, [86] demonstrated improved species discrimination accuracy because of the inclusion of the red edge and SWIR for Sentinel-2 data. This could provide an opportunity to locate the species regularly at the regional scale. However, numerous studies have noted that the spatial resolution of these sensors might complicate species mapping application, among other things due to spatial variability in the canopy. Findings in this paper are mainly based on simulated MSI Sentinel-2 and Landsat 8 OLI data. Therefore, there is a need to validate the findings here with real satellite and the respective field data.

4.3 Comparison of iECV-DA and RF-DA models

Both models were able to reduce the redundancy of the hyperspectral data while retaining the most useful information to carry out the discrimination classification. However, the results are shown in this study indicate that the classification results obtained from the RF-DA are slightly better than those obtained from the iECVA-DA classifier. It implies that the RF was able to reduce overlap in the spectra of some species and to extract meaningful information wavebands to attain high classification results. The performance of RF-DA (both scales) corroborates with other studies of plant species discrimination [87].

Similarly, [87] reported high accuracies and kappa statistics with RF-LDA when compared to typical RF classifier. In our case, at both the canopy scale, for example, the highest PPV, delineation accuracies of *A. mearnsii* was provided by RF-DA. However, there

was a relatively high amount of false positives and misclassification when compared to iECVA-DA classifier. Though these classifiers were successful in distinguishing *A. mearnsii*, it is essential to explore the validity of these models real field spectral reflectance of the plants.

The validity of the results from the simulated Landsat and Sentinel bands centres require evaluation using actual satellite images because the conditions of in-situ reflectance spectra data collection are different from that of the optical satellite images. For example, satellite image-based reflectance is affected by atmospheric effects, which is not the case with in-situ spectra data. Moreover, image spectral information is influenced by various environmental factors (e.g. micro-climate, soil characteristics, precipitation and topography), which causes spectral variance. Therefore, the demonstrated uniqueness of *A. mearnsii* spectra from that of sampled co-occurring native species requires validation at the regional level.

5. Conclusion

Methods of RS are powerful tools to characterise invasive species' distribution patterns. However, species characterisation using RS data is always hindered by strong spectral similarities between invasive species and other native plants. As a result, not all invasive species can be detected by RS data. It is critical to understand the limitations of the approach and to explore the prospect of detecting target species before incorporating the RS data in operational monitoring projects. This study investigated spectra separability between *A. mearnsii* and co-occurring species (*Celtis Africana, V. karoo, Dombeya tileacea, Olea Africana, Dombeya rotundifolia, V. xanthophloea, Euclea crispa*) within the South African landscape. The intention was to understand the spectral and seasonal variation between *A. mearnsii* and native species at leaf and canopy spectral level. The results of the study highlighted the following about the discrimination of *A. mearnsii.*

i. Invasive *A. mearnsii* can be distinguished from other species at leaf and canopy level using spectral reflectance

ii. Spectral differences related to senescence phenology (March and April) had a stronger effect on the separability between *A. mearnsii* and native species than other periods (December, January, February and May).

iii. Spectral regions associated with biochemical properties are essential in discriminating the species. For instance, there was high spectral separability in Red-edge and visible spectral regions at leaf and the canopy scales.

iv. A high spectral separability was yielded by using non-parametric RF-DA classifiers. The classifier was able to distinguish between *A. mearnsii* and sampled species even during the Southern Africa senescence-winter transition period (April-May).

v. Sentinel-2 MSI showed results comparable to Landsat-8 OLI regarding classifying *A. mearnsii* and studied native species.

This study can contribute to initiatives aimed at managing and monitoring invasive *A. mearnsii*. This research provides critical information towards an understanding of the spectral differences between *A. mearnsii* and co-occurring native species. The findings could be useful for understanding vital spectral bands required to delineate and monitor *A. mearnsii* in a mixed species environment.

Acknowledgements

Reference

[1] G.M. Luque, C. Bellard, C. Bertelsmeier, E. Bonnaud, P. Genovesi, D. Simberloff and F. Courchamp, "'The 100th of the world's worst invasive alien species," *Biol.Invasions*, vol. 16, no. 5, pp. 981-985.

[2] P. Pyšek, V. Jarošík, P.E. Hulme, J. Pergl, M. Hejda, U. Schaffner and M. Vilà, "'A global assessment of invasive plant impacts on resident species, communities and ecosystems: the interaction of impact measures, invading species' traits and environment," *Global Change Biol.*, vol. 18, no. 5, pp. 1725-1737.

[3] M. Rejmánek and D.M. Richardson, "'Trees and shrubs as invasive alien species–2013 update of the global database," *Divers.Distrib.*, vol. 19, no. 8, pp. 1093-1094.

[4] I. ISSG, "*International Union for the Conservation of Nature Invasive Species Specialist Group: 100 of the world's worst alien invasive species"*, Auckland: Invasive Species Specialist Group.

[5] M. Liu, M. Yang, D. Song, Z. Zhang and X. Ou, "'Invasive *Acacia mearnsii* De Wilde in Kunming, Yunnan Province, China: a new biogeographic distribution that Threatens Airport Safety," *NeoBiota*, vol. 29, pp. 53.

[6] J.L. Seburanga, "'Black Wattle (Acacia mearnsii De Wild.) in Rwanda's Forestry: Implications for Nature Conservation," *J.Sustainable For.*, vol. 34, no. 3, pp. 276-299.

[7] I. Boudiaf, E. Baudoin, H. Sanguin, A. Beddiar, J. Thioulouse, A. Galiana, Y. Prin, C. Le Roux, M. Lebrun and R. Duponnois, "'The exotic legume tree species, Acacia mearnsii, alters microbial soil functionalities and the early development of a native tree species, Quercus suber, in North Africa," *Soil Biol.Biochem.*, vol. 65, pp. 172-179.

[8] T.S. Yapi, P.J. O'Farrell, L.E. Dziba and K.J. Esler, "'Alien tree invasion into a South African montane grassland ecosystem: impact of Acacia species on rangeland condition and livestock carrying capacity," *International Journal of Biodiversity Science, Ecosystem Services & Management*, vol. 14, no. 1, pp. 105-116.

[9] T.S. Yapi, " *An assessment of the impacts of invasive Australian wattle species on grazing provision and livestock production in South Africa*", " PhD diss., Stellenbosch: Stellenbosch University.

[10] D.M. Richardson and M. Rejmánek, "'Trees and shrubs as invasive alien species–a global review," *Divers.Distrib.*, vol. 17, no. 5, pp. 788-809.

[11] F. Impson, C.A. Kleinjan, J.H. Hoffmann and J.A. Post, "'Dasineura rubiformis (Diptera: Cecidomyiidae), a new biological control agent for Acacia mearnsii in South Africa," *S.Afr.J.Sci.*, vol. 104, no. 7-8, pp. 247-249.

[12] H. Moyo and A.O. Fatunbi, "'Utilitarian perspective of the invasion of some South African biomes by Acacia mearnsii," *Global Journal of Environmental Research*, vol. 4, no. 1, pp. 6-17.

[13] D.C. Le Maitre, G.G. Forsyth, S. Dzikiti and M.B. Gush, "Estimates of the impacts of invasive alien plants on water flows in South Africa," *Water Sa*, vol. 42, no. 4, pp. 659-672.

[14] M.R. Lee, E.S. Bernhardt, P.M. Bodegom, J.H.C. Cornelissen, J. Kattge, D.C. Laughlin, Ü Niinemets, J. Peñuelas, P.B. Reich and B. Yguel, "Invasive species' leaf traits and dissimilarity from natives shape their impact on nitrogen cycling: a meta-analysis," *New Phytol.*, vol. 213, no. 1, pp. 128-139.

[15] J.K. Balch, B.A. Bradley, C.M. D'antonio and J. Gómez-Dans, " Introduced annual grass increases regional fire activity across the arid western USA (1980–2009)," *Global Change Biol.*, vol. 19, no. 1, pp. 173-183.

[16] M. Vila and I. Ibanez, "Plant invasions in the landscape," *Landscape Ecol.*, vol. 26, no. 4, pp. 461-472.

[17] B.A. Bradley, "Remote detection of invasive plants: a review of spectral, textural and phenological approaches," *Biol.Invasions*, vol. 16, no. 7, pp. 1411-1425.

[18] D.M. Richardson, J. Carruthers, C. Hui, F.A. Impson, J.T. Miller, M.P. Robertson, M. Rouget, J.J. Le Roux and J.R. Wilson, "Human-mediated introductions of Australian acacias–a global experiment in biogeography," *Divers.Distrib.*, vol. 17, no. 5, pp. 771-787.

[19] A.M. West, P.H. Evangelista, C.S. Jarnevich, S. Kumar, A. Swallow, M.W. Luizza and S.M. Chignell, "Using multi-date satellite imagery to monitor invasive grass species distribution in post-wildfire landscapes: An iterative, adaptable approach that employs open-source data and software," *International Journal of Applied Earth Observation and Geoinformation*, vol. 59, pp. 135-146.

[20] P.J. Weisberg, T.E. Dilts, O.W. Baughman, S.E. Meyer, E.A. Leger, K.J. Van Gunst and L. Cleeves, "Development of remote sensing indicators for mapping episodic die-off of an invasive annual grass (Bromus tectorum) from the Landsat archive," *Ecol.Ind.*, vol. 79, pp. 173-181.

[21] Z. Ouyang, Y. Gao, X. Xie, H. Guo, T. Zhang and B. Zhao, "Spectral discrimination of the invasive plant Spartina alterniflora at multiple phenological stages in a saltmarsh wetland," PloS One, vol. 8, pp. e67315, 201

[22] G.P. Asner, "12 Hyperspectral Remote Sensing of Canopy Chemistry, Physiology, and Biodiversity in Tropical Rainforests," *Hyperspectral remote sensing of tropical and sub-tropical forests*, pp. 261-296.

[23] B. Somers and G.P. Asner, "Hyperspectral time series analysis of native and invasive species in Hawaiian rainforests," *Remote Sensing*, vol. 4, no. 9, pp. 2510-2529.

[24] J.R.K. Lehmann, A. Große-Stoltenberg, M. Römer and J. Oldeland, "Field spectroscopy in the VNIR-SWIR region to discriminate between Mediterranean native plants and exotic-invasive shrubs based on leaf tannin content," *Remote Sensing*, vol. 7, no. 2, pp. 1225-1241.

[25] A. Große-Stoltenberg, C. Hellmann, C. Werner, J. Oldeland and J. Thiele, "Evaluation of continuous VNIR-SWIR spectra versus narrowband hyperspectral indices to discriminate the invasive Acacia longifolia within a Mediterranean dune ecosystem," *Remote Sensing*, vol. 8, no. 4, pp. 334.

[26] A. Große-Stoltenberg, C. Hellmann, J. Thiele, J. Oldeland and C. Werner, "Invasive acacias differ from native dune species in the hyperspectral/biochemical trait space," Journal of Vegetation Science, vol. 29, pp. 325-335, 2018.

[27] M.E. Andrew and S.L. Ustin, "'Spectral and physiological uniqueness of perennial pepperweed (Lepidium latifolium)," *Weed Sci.*, vol. 54, no. 6, pp. 1051-1062.

[28] C.A. Baldeck, M.S. Colgan, J. Féret, S.R. Levick, R.E. Martin and G.P. Asner, "Landscape-scale variation in plant community composition of an African savanna from airborne species mapping," *Ecol.Appl.*, vol. 24, no. 1, pp. 84-93.

[29] M.L. Clark and D.A. Roberts, "Species-level differences in hyperspectral metrics among tropical rainforest trees as determined by a tree-based classifier," *Remote Sensing*, vol. 4, no. 6, pp. 1820-1855.

[30] E.R. Hunt, J.H. Everitt and R. Hamilton, " A weed manager's guide to remote sensing and GIS-mapping and monitoring, Remote sensing applications center, USDA Forest Sevice, salt lake city, Utah." *USDA Forest Service Research Notes* (2005).

[31] M. Jiménez and R. Díaz-Delgado, "Towards a standard plant species spectral library protocol for vegetation mapping: A case study in the shrubland of Doñana National Park," *ISPRS International Journal of Geo-Information*, vol. 4, no. 4, pp. 2472-2495.

[32] D.C. Le Maitre, M. Gaertner, E. Marchante, E. Ens, P.M. Holmes, A. Pauchard, P.J. O'Farrell, A.M. Rogers, R. Blanchard and J. Blignaut, "Impacts of invasive Australian acacias: implications for management and restoration," *Divers.Distrib.*, vol. 17, no. 5, pp. 1015-1029.

[33] T.L. Morris, K.J. Esler, N.N. Barger, S.M. Jacobs and M.D. Cramer, "Ecophysiological traits associated with the competitive ability of invasive Australian acacias," *Divers.Distrib.*, vol. 17, no. 5, pp. 898-910.

[34] L. Henderson, "Invasive, naturalised and casual alien plants in southern Africa: a summary based on the Southern African Plant Invaders Atlas (SAPIA)," *Bothalia*, vol. 37, no. 2, pp. 215-248.

[35] B. Fu and K.B. Jones, "'Landscape ecology for sustainable environment and culture," Edited by K. Bruce Jones. New York: Springer, 2013.

[36] M.P. Ferreira, M. Zortea, D.C. Zanotta, Y.E. Shimabukuro and de Souza Filho, Carlos Roberto, "Mapping tree species in tropical seasonal semi-deciduous forests with hyperspectral and multispectral data," *Remote Sens.Environ.*, vol. 179, pp. 66-78.

[37] J. Féret and G.P. Asner, "Tree species discrimination in tropical forests using airborne imaging spectroscopy," *IEEE Trans.Geosci.Remote Sens.*, vol. 51, no. 1, pp. 73-84.

[38] G.P. Asner, M.O. Jones, R.E. Martin, D.E. Knapp and R.F. Hughes, "'Remote sensing of native and invasive species in Hawaiian forests," *Remote Sens.Environ.*, vol. 112, no. 5, pp. 1912-1926.

[39] M.C. Morais and H. Freitas, "Phenological dynamics of the invasive plant Acacia longifolia in Portugal," *Weed Res.*, vol. 55, no. 6, pp. 555-564.

[40] C. Huang and G.P. Asner, "'Applications of remote sensing to alien invasive plant studies," *Sensors*, vol. 9, no. 6, pp. 4869-4889.

[41] J.C. Doran and J.W. Turnbull, *Australian trees and shrubs: species for land rehabilitation and farm planting*. No. ACIAR Monograph no. 24. ACIAR, Canberra, Australia, 1997.

[42] B. Maslin and M. McDonald, "AcaciaSearch: evaluation of Acacia as a woody crop option for southern Australia," *Acacia Utilisation and Management–Adding Value*, vol. 26, pp. 86.

[43] G. Mukwada, W. Chingombe and P. Taru, "Critical considerations in Acacia mearnsii eradication: A case from South Africa," *Geographia Polonica*, vol. 89, no. 3, pp. 271-286.

[44] M. Strydom, R. Veldtman, M.Z. Ngwenya and K.J. Esler, "Invasive Australian Acacia seed banks: Size and relationship with stem diameter in the presence of gall-forming biological control agents," *PloS one*, vol. 12, no. 8, pp. e0181763.

[45] W. Ng, P. Rima, K. Einzmann, M. Immitzer, C. Atzberger and S. Eckert, "Assessing the Potential of Sentinel-2 and Pléiades Data for the Detection of Prosopis and Vachellia spp. in Kenya," *Remote sensing*, vol. 9, no. 1, pp. 74.

[46] G. Mallinis, I. Mitsopoulos and I. Chrysafi, "Evaluating and comparing Sentinel 2A and Landsat-8 Operational Land Imager (OLI) spectral indices for estimating fire severity in a

Mediterranean pine ecosystem of Greece," *GIScience & Remote Sensing*, vol. 55, no. 1, pp. 1-18.

[47] Z. Wang, "Mapping spatial variation of foliar nitrogen using hyperspectral remote sensing,"(2016).

[48] N. Mararakanye, M.N. Magoro, N.N. Matshaya, M.C. Rabothata and S.R. Ncobeni, "Railway side mapping of alien plant distributions in Mpumalanga, South Africa," *Bothalia-African Biodiversity & Conservation*, vol. 47, no. 1, pp. 1-11.

[49] M.A. Cho, R. Mathieu, G.P. Asner, L. Naidoo, J. van Aardt, A. Ramoelo, P. Debba, K. Wessels, R. Main, I.P.J. Smit and B. Erasmus, "Mapping tree species composition in South African savannas using an integrated airborne spectral and LiDAR system," *Remote Sens.Environ.*, vol. 125, pp. 214-226.

[50] O. Mutanga, A.K. Skidmore and S. van Wieren, "Discriminating tropical grass (Cenchrus ciliaris) canopies grown under different nitrogen treatments using spectroradiometry," *ISPRS Journal of Photogrammetry and Remote Sensing*, vol. 57, no. 4, pp. 263-272.

[51] M.A. Cho, A. Skidmore, F. Corsi, S.E. Van Wieren and I. Sobhan, "Estimation of green grass/herb biomass from airborne hyperspectral imagery using spectral indices and partial least squares regression," *International Journal of Applied Earth Observation and Geoinformation*, vol. 9, no. 4, pp. 414-424.

[52] A. Ramoelo, A.K. Skidmore, M. Schlerf, R. Mathieu and I.M. Heitkönig, "Water-removed spectra increase the retrieval accuracy when estimating savanna grass nitrogen and phosphorus concentrations," *ISPRS Journal of Photogrammetry and Remote Sensing*, vol. 66, no. 4, pp. 408-417.

[53] M.L. Clark, D.A. Roberts and D.B. Clark, "Hyperspectral discrimination of tropical rain forest tree species at leaf to crown scales," *Remote Sens. Environ.*, vol. 96, no. 3, pp. 375-398.

[54] I. Robinson and A. Mac Arthur, "the FSF post processing toolbox user guide," "The field spectroscopy facility post processing toolbox user guide." *Post processing spectral data in MATLAB, University of Edinburgh, Edinburgh, UK* (2011).

[55] A. Savitzky and M.J. Golay, "Smoothing and differentiation of data by simplified least squares procedures." *Anal.Chem.*, vol. 36, no. 8, pp. 1627-1639.

[56] T. Naes, T. Isaksson and B. Kowalski, "Locally weighted regression and scatter correction for near-infrared reflectance data," *Anal.Chem.*, vol. 62, no. 7, pp. 664-673.

[57] R.J. Barnes, M.S. Dhanoa and S.J. Lister, "Correction to the description of standard normal variate (SNV) and de-trend (DT) transformations in Practical Spectroscopy with Applications in Food and Beverage Analysis—2nd edition," *Journal of Near Infrared Spectroscopy*, vol. 1, no. 3, pp. 185-186.

[58] L.W. Lehnert, H. Meyer, W.A. Obermeier, B. Silva, B. Regeling and J. Bendix, "Hyperspectral Data Analysis in R: the hsdar Package," *arXiv preprint arXiv:1805.05090*.

[59] R Core Team (2018). R: A language and environment for statistical computing. R Foundation for Statistical Computing, Vienna, Austria. URL https://www.R-project.org/.

[60] L. Nørgaard, R. Bro, F. Westad and S.B. Engelsen, "'A modification of canonical variates analysis to handle highly collinear multivariate data," *A Journal of the Chemometrics Society 20, no. 8-10 (2006): 425-435*

[61] D.L. Jones, "The Fathom toolbox for MATLAB", *College of Marine Science, University of South Florida, St. Petersburg, FL* (2012).

[62] T.D. Lemmond, A.O. Hatch, B.Y. Chen, D. Knapp, L. Hiller, M. Mugge and W.G. Hanley, "Discriminant Random Forests.", In *Data Mining*, pp. 123-146. Springer, Boston, MA, 2010.

[63] L. Norgaard, A. Saudland, J. Wagner, J.P. Nielsen, L. Munck and S.B. Engelsen, "Interval partial least-squares regression (iPLS): a comparative chemometric study with an example from near-infrared spectroscopy," *Appl.Spectrosc.*, vol. 54, no. 3, pp. 413-419.

[64] R.O. Duda, P.E. Hart and D.G. S Stork. "Pattern classification and scene analysis". Vol. 3. New York: Wiley, 1973.

[65] J. Li, M. Tran and J. Siwabessy, "Selecting optimal random forest predictive models: A case study on predicting the spatial distribution of seabed hardness," *PloS one*, vol. 11, no. 2, pp. e0149089.

[66] Y.C. Saw, Z.I.M. Yusoh, A.K. Muda and A. Abraham, "Ensemble Filter-Embedded Feature Ranking Technique (FEFR) for 3D ATS Drug Molecular Structure,".

[67] W. Zhu, N. Zeng and N. Wang, "Sensitivity, specificity, accuracy, associated confidence interval and ROC analysis with practical SAS implementations," *NESUG proceedings: health care and life sciences, Baltimore, Maryland*, vol. 19.

[68] J.R. Landis and G.G. Koch, "The measurement of observer agreement for categorical data," *Biometrics*, pp. 159-174.

[69] A.H. Fielding and J.F. Bell, "A review of methods for the assessment of prediction errors in conservation presence/absence models," *Environ.Conserv.*, vol. 24, no. 1, pp. 38-49.

[70] P. Lurz, S.P. Rushton, L.A. Wauters, S. Bertolino, I. Currado, P. Mazzoglio and M. Shirley, "' Predicting grey squirrel expansion in North Italy: a spatially explicit modelling approach," *Landscape Ecol.*, vol. 16, no. 5, pp. 407-420.

[71] S. Madonsela, M.A. Cho, R. Mathieu, O. Mutanga, A. Ramoelo, Ż Kaszta, R. Van De Kerchove and E. Wolff, "Multi-phenology WorldView-2 imagery improves remote sensing of savannah tree species," *International Journal of Applied Earth Observation and Geoinformation*, vol. 58, pp. 65-73.

[72] M.A. Cho, J. Van Aardt, R. Main and B. Majeke, "Evaluating variations of physiology-based hyperspectral features along a soil water gradient in a Eucalyptus grandis plantation," *Int.J.Remote Sens.*, vol. 31, no. 12, pp. 3143-3159.

[73] K.W. Tomlinson, L. Poorter, F.J. Sterck, F. Borghetti, D. Ward, S. Bie and F. Langevelde, "Leaf adaptations of evergreen and deciduous trees of semi-arid and humid savannas on three continents," *J.Ecol.*, vol. 101, no. 2, pp. 430-440.

[74] K. Bai, C. He, X. Wan and D. Jiang, "Leaf economics of evergreen and deciduous tree species along an elevation gradient in a subtropical mountain," AoB Plants 7, vol. 7, 2015.

[75] G.A. Blackburn, "Hyperspectral remote sensing of plant pigments," *Journal of experimental botany 58, no. 4 (2006): 855-867.*

[76] J.G. Ferwerda and S.D. Jones, "'Continuous wavelet transformations for hyperspectral feature detection," In *Progress in spatial data handling*, pp. 167-178. Springer, Berlin, Heidelberg, 2006.

[77] K. Bhosle and V. Musande, "Stress Monitoring of Mulberry Plants by Finding Rep Using Hyperspectral Data," *The International Archives of Photogrammetry, Remote Sensing and Spatial Information Sciences* 42 (2017): 383.

[78] R. Main, M.A. Cho, R. Mathieu, M.M. O'Kennedy, A. Ramoelo and S. Koch, "An investigation into robust spectral indices for leaf chlorophyll estimation," ISPRS Journal of Photogrammetry and Remote Sensing, vol. 66, pp. 751-761, 2011.

[79] M.A. Cho, I. Sobhan, A.K. Skidmore and J. De Leeuw, "Discriminating species using hyperspectral indices at leaf and canopy scales," *The International Archives of the Photogrammetry, Remote Sens." Spatial Inform. Sci.*, XXXVII. Part B7 (2008). [80] M. Kalacska, S. Bohlman, G.A. Sanchez-Azofeifa, K. Castro-Esau and T. Caelli, "Hyperspectral discrimination of tropical dry forest lianas and trees: Comparative data reduction approaches at the leaf and canopy levels." *Remote Sensing of Environment* 109, no. 4 (2007): 406-415.

[81] G. Weil, I.M. Lensky, Y.S. Resheff and N. Levin, "Optimizing the Timing of Unmanned Aerial Vehicle Image Acquisition for Applied Mapping of Woody Vegetation Species Using Feature Selection," *Remote Sensing 9, no. 11 (2017): 1130.*

[82] M. Niphadkar and H. Nagendra, "'Remote sensing of invasive plants: incorporating functional traits into the picture," *Int.J.Remote Sens.*, vol. 37, no. 13, pp. 3074-3085.

[83] C. Sothe, C.M.d. Almeida, V. Liesenberg and M.B. Schimalski, "Evaluating Sentinel-2 and Landsat-8 Data to Map Sucessional Forest Stages in a Subtropical Forest in Southern Brazil," *Remote Sensing*, vol. 9, no. 8, pp. 838.

[84] A. Ramoelo and M.A. Cho, " Explaining Leaf Nitrogen Distribution in a Semi-Arid Environment Predicted on Sentinel-2 Imagery Using a Field Spectroscopy Derived Model," *Remote Sensing*, vol. 10, no. 2, pp. 269.

[85] A. Ramoelo, M. Cho, R. Mathieu and A.K. Skidmore, "Potential of Sentinel-2 spectral configuration to assess rangeland quality," *Journal of applied remote sensing*, vol. 9, no. 1, pp. 094096.

[86] S. Adelabu, O. Mutanga and E. Adam, "Evaluating the impact of the red-edge band from Rapideye image for classifying insect defoliation levels," *ISPRS Journal of Photogrammetry and Remote Sensing*, vol. 95, pp. 34-41.

[87] A. Gholizadeh, M. Saberioon, L. Borůvka, A. Wayayok and M.A.M. Soom, "Leaf chlorophyll and nitrogen dynamics and their relationship to lowland rice yield for site-specific paddy management," Information Processing in Agriculture, vol. 4, pp. 259-268, 2017.

[88] K. Prospere, K. McLaren and B. Wilson, "Plant species discrimination in a tropical wetland using in situ hyperspectral data," *Remote sensing*, vol. 6, no. 9, pp. 8494-8523.

[89] A. Große-Stoltenberg, C. Hellmann, J. Thiele, C. Werner and J. Oldeland, "Early detection of GPP-related regime shifts after plant invasion by integrating imaging spectroscopy with airborne LiDAR," Remote Sens.Environ., vol. 209, pp. 780-792, 2018.

[90] Breiman, Leo. "Random forests." *Machine learning* 45, no. 1 (2001): 5-32.